MEDIUM MODIFICATIONS OF HADRONS STUDIED WITH PHOTONUCLEAR REACTIONS* **

S. Schadmand

for the TAPS and the A2 Collaborations

II Physikalisches Institut, Justus Liebig Universität Giessen
Heinrich Buff Ring 16, 35392 Giessen, Germany

(Received January 22, 2002)

The experiments with the electromagnetic calorimeter TAPS using tagged photon beams focus on meson production from the free proton and from nucleons bound in nuclei. Following an introduction, results from the recent TAPS campaign at the tagged photon facility MAMI (Mainz) on double pion photo-production are presented. The observations using a proton target provide direct evidence for a ρ strength in the decay of the D_{13} resonance. Furthermore, double pion production from nuclei is used as a tool to study in-medium modifications of the $\pi\pi$ interaction which might indicate a partial restoration of chiral symmetry.

PACS numbers: 13.60.Le, 14.20.Gk, 25.20.Lj

1. Introduction

Nucleons are composite particles containing quarks and gluons. The complex nucleon structure manifests itself in a rich excitation spectrum exhibiting several nucleon resonances. This can be seen in Fig. 1 where the total photo-absorption cross section on the proton is seen to have resonance structure. Three resonance regions are observed. The first, around $E_\gamma = 330\,\mathrm{MeV}$, contains the lowest excitation state, a P_{33} resonance, called the Δ resonance. Two more resonance regions are observed at higher energies, the second and third resonance regions, each consisting of several overlapping resonant states.

* Presented at the VI TAPS Workshop, Krzyże, Poland, September 9–13, 2001.
** This work was supported by Deutsche Forschungsgemeinschaft (SFB 201) and the U.K. Engineering and Physical Sciences Research Council.

Nucleon resonances are short-lived and decay via the emission of mesons. Therefore, a more detailed investigation requires the study of meson production. The left panel of Fig. 1 shows the decomposition of the photo-absorption cross section on the proton into single and double meson production. In photo-absorption as well as single π^0 production, the identification

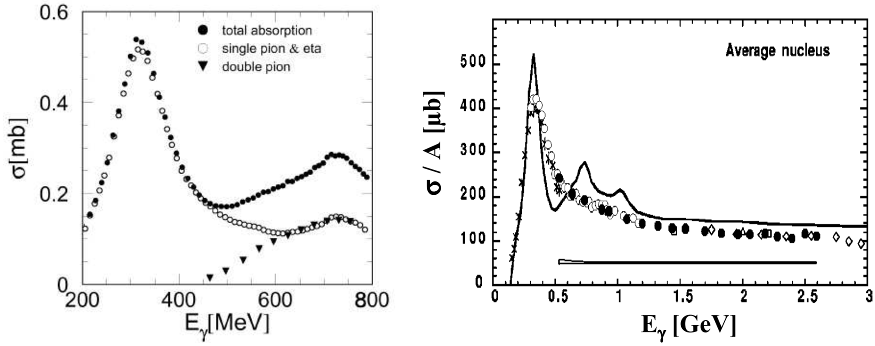

Fig. 1. Total photo-absorption cross section on the proton and decomposition into single and double meson production reactions (left). Comparison of photo-absorption cross sections on the proton (solid line) and nuclei, taken from [2] (right).

of the individual resonances is hindered by their large widths and strong overlap with each other. However, a separation of the resonances in the second resonance region is possible via their characteristic decay into two π and into η mesons. Fig. 2 gives an overview of the nucleon excitation spectrum and the characteristic decay modes of the resonances. The excitation spectrum shows nucleon resonances accessible with beam energies as provided by the tagged photon beam facility at the MAMI electron accelerator. Here, the second resonance region with $M(N^{\star})$=1400–1600 MeV is covered. The $P_{11}(1440)$, $S_{11}(1535)$, and $D_{13}(1520)$ resonances are contributing to this region. The notation originates from pion scattering experiments on the proton where the angular momentum L refers to the relative angular momentum between the pion and the proton. The resonance properties and decay modes are listed in Table I. Characteristic decays are $P_{11} \to N\pi\pi$, $D_{13} \to N\pi\pi$, and $S_{11}(1535) \to N\eta$, as can be seen from the probabilities for the various decay modes. The information quoted in [1] has been extracted by means of coupled channel analyses.

A comparison of photo-absorption cross sections on the proton and on nuclei in the right panel of Fig. 1 shows strong differences in the second resonance region [2]. The resonance structure is prominent in photo-absorption on the free nucleon and appears strongly suppressed for photo-absorption on nuclei. In this energy region, the $D_{13}(1520)$ resonance is dominantly excited in photoproduction and an in-medium broadening of this resonance could be the cause of the observations. The broadening would arise from coupling the resonance to the $N\rho$ final state [3,4] where the ρ meson itself is appreciably broadened in the nuclear medium [5]. This scenario is based on a substantial ρ-decay width of the D_{13} resonance which should be observable on the free proton. The ρ-decay width of the free D_{13} resonance is quoted by the Particle Data Group [1] and Manley [6]. However, the parameters were extracted from coupled channel analyses of pion induced reactions and the decay channel was not directly observed. Indications for ρ strength in photo-absorption experiments have been deduced by the DAPHNE group in the $\gamma n \to \pi^- - \pi^0 p$ reaction on a deuteron target [7] by comparison to model calculations of Ochi *et al.* [8]. In the experimental analysis, effects stemming from the fact that the neutron is bound in the deuteron target had to be accounted for. In Sec. 3, the TAPS results on the first direct observation of the ρ strength from the reaction $\gamma + p$ [9] are reported.

The study of double pion production is extended to nucleons embedded in nuclei in order to investigate in-medium modifications of the $\pi\pi$ interaction which might indicate a partial restoration of chiral symmetry [11–13]. The results of pion-induced experiments $(\pi^+, \pi^+\pi^-)$ [14] and $(\pi^-, \pi^0\pi^0)$ [15] could be interpreted in that sense. Photon-induced reactions can reach higher nuclear densities and should be more sensitive to in-medium effects. In Sec. 4, the TAPS study of the reactions $\gamma + A \to \pi^0\pi^0 + X$ with $A = p$, D, C and Pb is discussed.

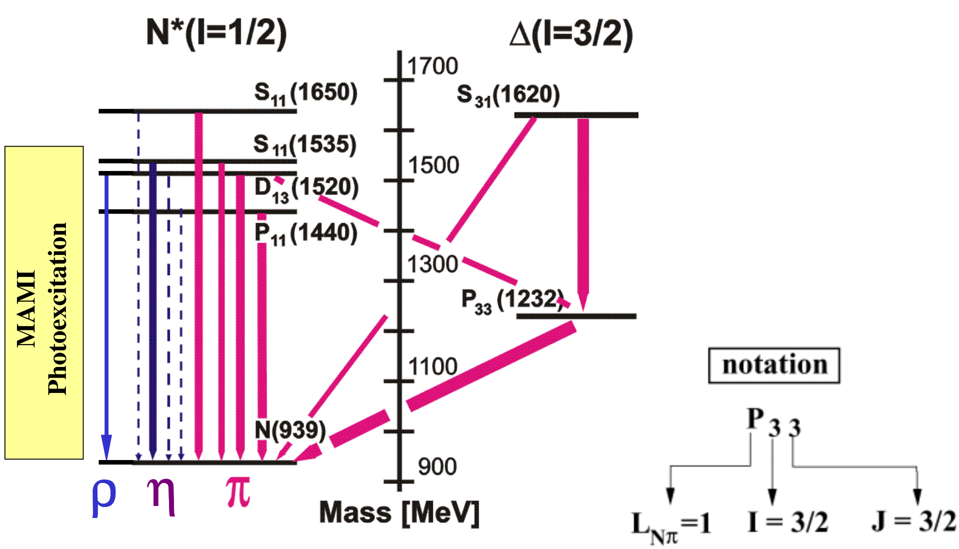

Fig. 2. Overview of the nucleon excitation spectrum and the characteristic decay modes of the resonances.

TABLE I

Resonances contributing to the second resonance region and their decay properties according to [1]. The resonances decay to about 50% via single pion emission. Characteristic decays are $P_{11} \to N\pi\pi$, $D_{13} \to N\pi\pi$, and $S_{11}(1535) \to N\eta$.

Resonance $N^\star(M)$	Width	Decay mode	Decay probability
$P_{11}(1440)$	350 MeV	$N\pi$	60–70%
		$N\pi\pi$	30–40%
		$\Delta\pi$	20–30%
		$N\rho$	<8%
		$N(\pi\pi)^{l=o}_{s-\text{wave}}$	5–10%
$D_{13}(1520)$	120 MeV	$N\pi$	50–60%
		$N\pi\pi$	40–50%
		$\Delta\pi$	15–25%
		$N\rho$	15–25%
		$N(\pi\pi)^{l=o}_{s-\text{wave}}$	<8%
$S_{11}(1535)$	150 MeV	$N\pi$	35–55%
		$N\eta$	30–55%
		$N\pi\pi$	1–10%

2. Experimental setup

The experiments were performed with the TAPS detector [16] in combination with the Glasgow tagged photon beam facility [17] at the MAMI accelerator in Mainz [18]. Six detector blocks consisting of 64 BaF_2 plastic telescopes, respectively, and a forward wall of 120 telescopes were arranged in a plane around the scattering chamber. The detection system provides time-of-flight, energy, and pulse shape information of the detected particles. In addition, neutral/charged particle identification can be derived from thin plastic scintillators in front of the BaF_2 crystals. In the experimental campaign, quasi-monochromatic photons up to 850 MeV were employed. $\pi^0\pi^0$ and $\pi^+\pi^0$ data were simultaneously acquired using the same detection system and similar analysis. π^0 and η mesons are identified via their 2 photon decay using an invariant mass analysis and charged pions via time-of-flight. The studies are performed on the free proton as well as on nucleons bound in nuclei.

3. Double pion photoproduction on the proton

Fig. 3 shows the total cross section of the reaction $\gamma p \to \pi^+\pi^0 n$ and $\gamma p \to \pi^0\pi^0 p$ as a function of the incident photon energy. The TAPS results (filled and open circles) are compared to theoretical predictions of [19] (solid curve). In both panels of Fig. 3, dashed curves represent the theoretical result without a ρ contribution [20]. The TAPS result is consistent with a previous measurement performed with the DAPHNE detector (open squares) [21] confirming the resonance structure at the $D_{13}(1520)$ resonance (E_γ=760 MeV). $\pi\pi$ production proceeds to a large extent through the sequential decay of the $D_{13}(1520)$ (E_γ = 760 MeV) via the $\Delta(1232)$ resonance [22]. $N\pi$ invariant mass distributions from the present data set indicate that a sequential decay is also important in the $\pi^+\pi^0$ channel [9]. This is in agreement with the assumption of Refs. [20, 23] and can be seen in Fig. 3 by comparing the experimental data and the dashed curves (without ρ). The structure in the $\pi^+\pi^0$ cross section is explained by an interference of the $D_{13} \to N\rho$-decay with the ρ Kroll–Rudermann contribution [19], both indicated separately (short-dashed and dotted curves), and indicates the importance of a ρ contribution.

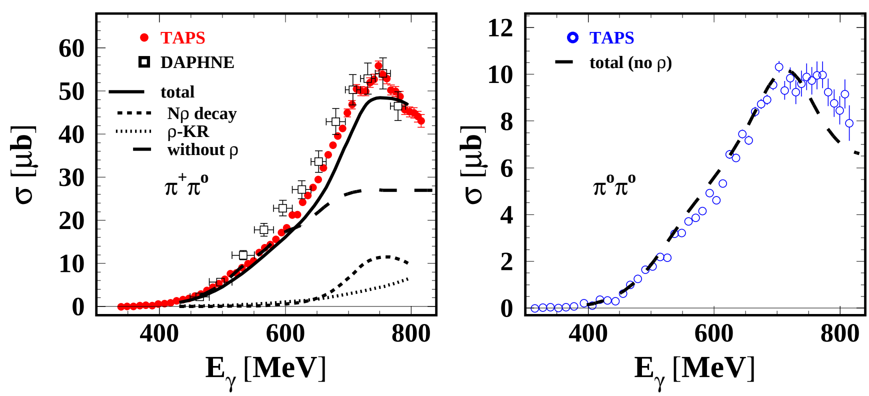

Fig. 3. $\pi^+\pi^0$ [9] (left) and $\pi^0\pi^0$ [22] total photoproduction cross section from the proton as a function of incident photon energy (right).

The statistics of the TAPS results allow to directly compare $\pi\pi$ invariant mass distributions from the reactions $\gamma p \to \pi^+\pi^0 n$ and $\gamma p \to \pi^0\pi^0 p$ [9]. The $\rho \to \pi\pi$ contribution can be observed in the $\pi^+\pi^0$ invariant mass distributions but the ρ-meson decay into $\pi^0\pi^0$ is forbidden. Therefore, deviations of $\pi^+\pi^0$ from $\pi^0\pi^0$ invariant mass distributions are regarded as a measure of the ρ contribution. Fig. 4 shows $\pi\pi$ invariant mass distributions for the $\pi^0\pi^0$ and $\pi^+\pi^0$ reactions on the proton. At low excitation energies both experimental distributions agree within the error bars with phase space. Apart from pure phase space contributions, this low energy behavior is connected to the contribution of the sequential decay of the D_{13} resonance which provides a featureless distribution similar to a phase space distribution. In the second resonance region the $\pi^+\pi^0$ system shows a pronounced shift to higher masses. As pointed out above, the ρ^0 meson cannot decay into $2\pi^0$. The deviation towards higher invariant masses in the charged channel is attributed to an intermediate ρ^+ meson. Here, the low energy tail of the broad ρ meson of mass 770 MeV and full width 150 MeV is populated. The right hand side of Fig. 4 shows a comparison of the mass distributions to the calculations

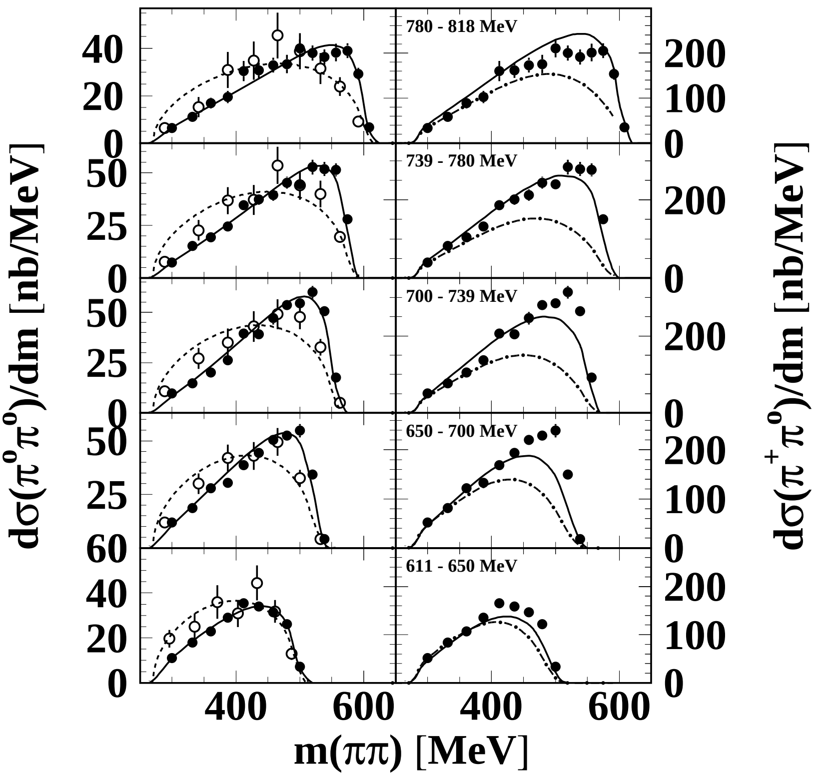

Fig. 4. Invariant mass distributions of pion pairs from the proton for five bins of incident photon energy. Comparison of the shape of the distributions for $\gamma p \to \pi^+\pi^0 n$ (solid circles) and $\gamma p \to \pi^0\pi^0 p$ (open circles). Dashed curve: phase space expectation, full curve: fit to the $\pi^+\pi^0$ data [9]. The vertical scale corresponds to the $\pi^0\pi^0$ data, the $\pi^+\pi^0$ data and the curves are normalized to the same area (left). Comparison of the $\pi^+\pi^0$ distributions to the calculations with (solid line) [19] and without (dash-dotted line) [20] ρ contributions (right).

with and without the inclusion of the $D_{13} \to N\rho$- and ρ-Kroll–Rudermann decays, using the PDG-values for masses and widths [1]. The deviations are assigned to a ρ branch of the $D_{13}(1520)$ resonance since this state is predominantly excited in the second resonance region and the $\pi^+\pi^0$ cross section in Fig. 3 shows a broad peak at the $D_{13}(1520)$ resonance (E_γ=760 MeV, $\Gamma_{D_{13}} = 120$ MeV).

This conclusion is supported by a simplified fit to the data considering a phase space contribution (representing sequential decays in approximation) and a ρ contribution as in $\gamma p \to \rho^+ n \to \pi^+\pi^0 n$. The fit is explained in more detail in [9]. The ratio of squared ρ channel and phase space amplitudes deduced from the fit to the $\pi^+\pi^0$ data is shown in Fig. 5. The ratio, plotted

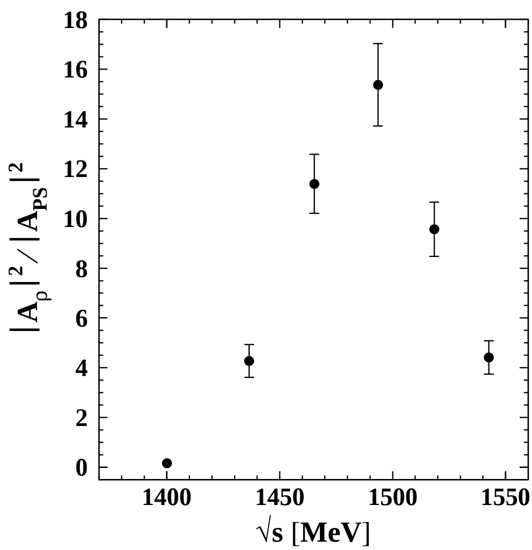

Fig. 5. Ratio of squared ρ channel and phase space amplitudes deduced from the fit to the $\pi^+\pi^0$ data from the proton as in Fig. 4.

as a function of the center of mass energy $\sqrt{s}$, is a measure of ρ contributions and exhibits a resonance structure near the mass pole of the $D_{13}(1520)$ resonance. The result that the D_{13} resonance has a substantial ρ-decay branch is confirmed by the rigorous theoretical treatment of double pion photoproduction [19] which has been motivated by this experiment. Here, the cross section is reproduced for a branching ratio of 20% for the $D_{13} \to N\rho$ channel.

4. In-medium double pion photoproduction

The elusive σ meson is assumed to be an isoscalar–scalar $\pi\pi$ state ($J^P = 0^+$) and is quoted to have a mass of 500–1200 MeV in the vacuum [1]. This meson would be considered a tool to investigate chiral symmetry restoration as it has the same quantum numbers as the QCD vacuum. Partial restoration of chiral symmetry is expected to be progressing with increasing baryon density or temperature and would lead to a dropping of the σ mass [10], reaching the π mass in the case of full chiral symmetry restoration. The π meson, being a Goldstone boson, does not experience such drastic mass changes.

The dropping of the σ mass should be observable via its decay into pion pairs. Here, the $\pi\pi$ invariant mass distributions should exhibit a shift towards the two-pion threshold with increasing baryon density [11–13]. This signature of partial chiral symmetry restoration is expected to set in already at normal nuclear density. However, the observed pions may experience final state interactions and appropriate care has to be taken in the interpretation of the results.

In the TAPS photoproduction experiments at MAMI, the reactions $\gamma + A \rightarrow \pi^0\pi^0 + X$ with $A = p$, D, C and Pb were studied. The coherent production cross section is negligible and the investigation deals with nucleons embedded in nuclei. The incident photon energy was chosen to be 400–460 MeV in order to keep the sum of the pion kinetic energies below 100 MeV, thereby minimizing pion final state interactions. From the proton to the carbon and to the lead target, the resulting $\pi^0\pi^0$ mass distributions, as seen in Fig. 6, exhibit a gradual mass shift towards small invariant masses, as would be expected from theoretical predictions of chiral symmetry restoration. For the carbon target, good agreement is found with the $\pi^0\pi^0$ data measured with the Crystal Ball using pion beams [15]. The results are compared to $\pi^+\pi^0$ distributions in order to judge the influence of final state interactions. The $\pi^+\pi^0$ production channel, carrying isospin $I = 1$, cannot stem from the σ meson decay but the charged pions undergo final state interactions similar to neutral pions. The $\pi^+\pi^0$ distributions do not exhibit the same mass shift. It can be concluded that final state interactions of the produced pions play a minor role at these energies. The observed shift in the $\pi^0\pi^0$ mass distributions is consistent with the prediction of partial chiral symmetry restoration at normal nuclear density. This result confirms earlier measurements by the CHAOS collaboration with pion beams [14] which were hampered in their quantitative interpretation by acceptance issues.

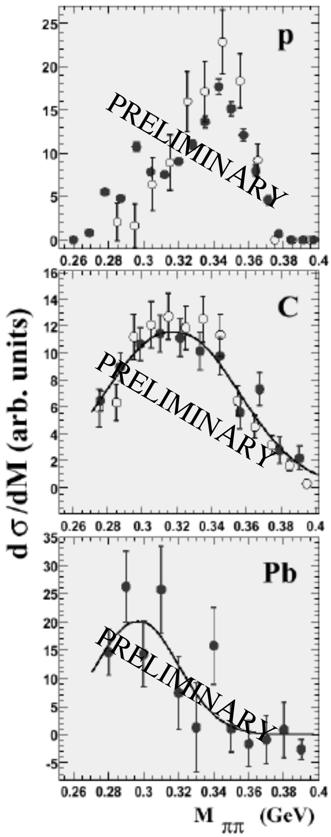

Fig. 6. Preliminary TAPS $\pi^0\pi^0$ invariant mass distributions (solid circles) for various targets at 400–460 MeV incident photon energies. The data are normalized for comparison with the Crystal Ball results (open circles). Solid curves are fits to the TAPS points.

5. Summary

The $\pi\pi$ photo-production from the proton up to 820 MeV excitation energy has been discussed. Here, the $\pi^+\pi^0$ system has been compared to simultaneously measured $\pi^0\pi^0$ data for production on the free nucelon as well as on nucleons embedded in nuclei.

For the proton the $\pi^+\pi^0$ invariant mass distributions are shifted towards higher masses. This behavior provides first experimental evidence for a contribution of an intermediate ρ^+ meson with a subsequent decay into two pions in the reaction $\gamma\, p \to \rho^+\, n \to \pi^+\pi^0\, n$. Because of the resonant behavior this ρ strength is assigned to the decay of the $D_{13}(1520)$ resonance as also found in recent calculations by Nacher *et al.* [19]. The ρ-decay branch of the $D_{13}(1520)$ is of great interest for the understanding of medium modifications in nuclear reactions. A strong broadening of the ρ spectral function should have an impact on the decaying resonance and might play a role in the depletion of the nuclear photo-absorption cross section in the second resonance region.

The TAPS results on double pion photoproduction from nuclei are used as a tool to study a possible signature of partial chiral symmetry restoration. In contrast to previous pion-induced measurements, photon-induced reactions avoid absorption of the incident probe on the nuclear surface. The mass distributions show a shift in the $\pi^0\pi^0$ invariant mass distributions towards small invariant masses which is not observed in the $\pi^+\pi^0$ channel. The shift increases gradually as a function of target mass number. It is consistent with theoretical expectations of partial chiral symmetry restoration and the corresponding signature of a dropping σ mass.

REFERENCES

[1] C. Caso *et al.*, *Eur. Phys. J.* **C3**, (1998).
[2] V. Muccifora *et al.*, *Phys. Rev.* **C60**, 064616 (1999) and references therein.
[3] M. Effenberger *et al.*, *Phys. Rev.* **C60**, 044614 (1999).
[4] U. Mosel *et al.*, *Prog. Part. Nucl. Phys.* **42**, 163 (1999).
[5] F. Klingl *et al.*, *Nucl. Phys.* **A624**, 527 (1997).
[6] D.M. Manley, E.M. Saleski, *Phys. Rev.* **D45**, 4002 (1992).
[7] A. Zabrodin *et al.*, *Phys. Rev.* **C60**, 055201 (1999).
[8] K. Ochi *et al.*, *Phys. Rev.* **C56**, 1472 (1997); K. Ochi *et al.*, `nucl-th/9711031`.
[9] W. Langgärtner *et al.*, *Phys. Rev. Lett.* **87**, 052001 (2001).
[10] V. Bernard *et al.*, *Phys. Rev. Lett.* **59**, 966 (1987).
[11] T. Hatsuda *et al.*, *Phys. Rev. Lett.* **82**, 2840 (1999).
[12] P. Schuck *et al.*, `nucl-th/0002031`; Hirschegg 2001, Hadrons in dense matter, 73–79
[13] R. Rapp *et al.*, *Phys. Rev.* **C59**, 1237 (1999).
[14] F. Bonutti *et al.*, *Phys. Rev. Lett.* **77**, 603 (1996).
[15] A. Starostin *et al.*, *Phys. Rev. Lett.* **85**, 5539 (2000).
[16] R. Novotny, *IEEE Trans. Nucl. Sci.* **38**, 379 (1991).
[17] I. Anthony *et al.*, *Nucl. Instrum. Methods Phys. Res.* **A301**, 230 (1991).
[18] Th. Walcher, *Prog. Part. Nucl. Phys.* **24**, 189 (1990).
[19] J.C. Nacher *et al.*, *Nucl. Phys.* **A695**, 295 (2001).
[20] J.A. Gómez Tejedor, E. Oset, *Nucl. Phys.* **A600**, 413 (1996).
[21] A. Braghieri *et al.*, *Phys. Lett.* **B363**, 46 (1995).
[22] M. Wolf *et al.*, *Eur. Phys. J.* **A9**, 5 (2000).
[23] L.Y. Murphy, J.M. Laget, DAPNIA/SPhN **96**, (1996).